Atmos. Meas. Tech. Discuss., 6, 3581–3610, 2013
www.atmos-meas-tech-discuss.net/6/3581/2013/
doi:10.5194/amtd-6-3581-2013

Atmospheric Measurement Techniques Discussions

Implementation of a 3-D-Var system for atmospheric profiling data assimilation into the RAMS model: initial results

S. Federico

ISAC-CNR, UOS of Rome, Rome (RM), Italy

Received: 3 March 2013 – Accepted: 29 March 2013 – Published: 12 April 2013

Correspondence to: S. Federico (s.federico@isac.cnr.it)

Published by Copernicus Publications on behalf of the European Geosciences Union.

Abstract

This paper presents the current status of development of a three-dimensional variational data assimilation system. The system can be used with different numerical weather prediction models, but it is mainly designed to be coupled with the Regional Atmospheric Modelling System (RAMS). Analyses are given for the following parameters: zonal and meridional wind components, temperature, relative humidity, and geopotential height.

Important features of the data assimilation system are the use of incremental formulation of the cost-function, and the use of an analysis space represented by recursive filters and eigenmodes of the vertical background error matrix. This matrix and the length-scale of the recursive filters are estimated by the National Meteorological Center (NMC) method.

The data assimilation and forecasting system is applied to the real context of atmospheric profiling data assimilation, and in particular to the short-term wind prediction. The analyses are produced at 20 km horizontal resolution over central Europe and extend over the whole troposphere. Assimilated data are vertical soundings of wind, temperature, and relative humidity from radiosondes, and wind measurements of the European wind profiler network.

Results show the validity of the analysis solutions because they are closer to the observations (lower RMSE) compared to the background (higher RMSE), and the differences of the RMSEs are consistent with the data assimilation settings.

To quantify the impact of improved initial conditions on the short-term forecast, the analyses are used as initial conditions of a three-hours forecast of the RAMS model. In particular two sets of forecasts are produced: (a) the first uses the ECMWF analysis/forecast cycle as initial and boundary conditions; (b) the second uses the analyses produced by the 3-D-Var scheme as initial conditions, then is driven by the ECMWF forecast.

AMTD
6, 3581–3610, 2013

The improvement is quantified by considering the horizontal components of the wind, which are measured at a-synoptic times by the European wind profiler network. The results show that the RMSE is effectively reduced at the short range (1–2 h). The results are in agreement with the set-up of the numerical experiment.

1 Introduction

Modern numerical weather prediction (NWP) data assimilation systems use information from a range of sources to provide the best estimate of the atmospheric state, i.e. the analysis, at a given time. These systems combine information coming from the observations, an a-priori estimate of the atmospheric state (the background or first-guess field), detailed error statistics, and the law of physics.

Nowadays, increased computing power coupled with greater access to real-time a-synoptic data is paving the way toward a new generation of high-resolution (i.e. on the order of 10 km or less) operational mesoscale analyses and forecast systems (Kalnay, 2003; Barker et al., 2003a; Lazarus, 2002). Moreover, better initial conditions are increasingly considered of the utmost importance for a range of NWP applications, in particular at the short range (0–12 h, Zhang et al., 2005; Scenkman et al., 2011).

The variational data assimilation systems have the advantage to assimilate quantities not trivially related to the standard atmospheric variables, as radiances, and they include the imposition of dynamic balance either by the model itself (4-D-Var) or through the explicit use of balance equations. In recent years, these advantages have fostered the implementation of variational data assimilation systems in limited area models (Barker et al., 2003a; Xiang-Yu et al., 2009; Zupanski et al., 2005). These systems replaced previously used scheme as, for example, optimal interpolation (Parrish and Derber, 1992; Rabier et al., 2000).

This paper shows the development of a three-dimensional stand-alone data assimilation system tailored to be used with the Regional Atmospheric Modeling System (RAMS; Cotton et al., 2003; Pielke, 2002). In particular, the data assimilation system

AMTD
6, 3581–3610, 2013

can use the RAMS field as background and the analyses can be used to initialize the RAMS model.

The main features of the analysis system are:

1. Incremental formulation of the cost-function (Courtier et al., 1994), i.e. observations are assimilated to provide analysis increments. In this way, the analysis imbalance is kept at minimum as the first guess, to which the increments are added, is already balanced because it comes from the output of a numerical model.

2. Preconditioning of the background cost function through a control variable transformation **U** defined as $\mathbf{B} = \mathbf{U}\mathbf{U}^{\mathrm{T}}$, where **B** is the background error covariance matrix. Background error covariances are estimated by the Parrish and Derber method (Parrish and Derber, 1992), also known as the National Meteorological Center (NMC) method.

3. Control variables are the two components of the horizontal wind, temperature and relative humidity. The geopotential height is retrieved from the increments of the horizontal wind through the geostrophic balance. This ensures the balance between the mass and wind field increments. Moreover, the formulation permits to easily include more advanced balance equations in future implementations, as for example including the cyclostrophic flow and the friction. This will further extend the use of the data assimilation system in regions where the geostrophic balance is a poor approximation of the real atmospheric flow.

4. The horizontal component of the background error is represented through isotropic and homogeneous recursive filters. The vertical component of the background error is represented through decomposition into climatologically averaged (in time, longitude and latitude) eigenvectors of the vertical error, which is computed by the NMC method.

5. The minimization of the cost-function is performed by a conjugate-gradient algorithm (Press et al., 1993), which uses parallel directives.

AMTD
6, 3581–3610, 2013

This paper presents an upgrade of the 2-D-Var data assimilation system reported in Federico (2013). Two important features are introduced: (a) the use of the 3-D-Var method, which replaces the 2-D-Var; (b) the option to run the analysis on the same horizontal coordinate system of the RAMS model, which simplifies the interaction between the analysis and RAMS.

It is important to mention that a 4-D-Var data assimilation system is already in use for RAMS (Zupanski et al., 2005; Polkinghorne et al., 2009). Nevertheless the aim of this work is to realize a simple but effective variational system, suitable for application and operational implementation in small meteorological centres. The 3-D-Var, indeed, requires less computational resources compared to 4-D-Var (Rabier et al., 2000) or Ensemble Kalman filters (Anderson, 2001). It does not require the adjoint model and is simpler to implement. Moreover, the 3-D-Var system can be effective at improving the initial model state and has the advantages of variational data assimilation systems.

Even if the data assimilation system is continuously under development, it proves to be fast and reliable and can be used for real applications. So, while the basic aim of the paper is to show the general characteristics of the 3-D-Var scheme, an application to the data assimilation of tropospheric profiles is given. It is also noticed that the numerical experiment set-up of this paper should be of interest for the atmospheric profiling community because it can be used in OSE (Observing System Experiment), which allows for the objective assessment and comparison of existing observing systems, or in OSSE (Observing System Simulation Experiment), whose aim is to show the impact of next generation observing systems in a controlled software environment as, for example, weather prediction models (Otkin et al., 2011; Moninger et al., 2010).

The paper is divided as follows: Sect. 2 provides details about the data assimilation system; Sect. 3 shows the numerical experiment set-up; Sect. 4 gives the results of the application to the short-term wind forecast, and Sect. 5 gives conclusions.

AMTD
6, 3581–3610, 2013

2 The data assimilation system

The basic goal of the 3-D-Var algorithm is to produce an optimal estimate of the true atmospheric state at analysis time through iterative solution of a prescribed cost-function (Ide et al., 1997):

$$J(\boldsymbol{x}) = \frac{1}{2}(\boldsymbol{x}-\boldsymbol{x}_\mathrm{b})^\mathrm{T}\mathbf{B}^{-1}(\boldsymbol{x}-\boldsymbol{x}_\mathrm{b}) + \frac{1}{2}(\boldsymbol{y}_\mathrm{o}-H(\boldsymbol{x}))^\mathrm{T}\mathbf{R}^{-1}(\boldsymbol{y}_\mathrm{o}-H(\boldsymbol{x})) \quad (1)$$

where $J(\boldsymbol{x})$ is the cost-function, $\boldsymbol{x}$ is the state vector, $\boldsymbol{x}_\mathrm{b}$ is the background state, H is the forward observational operator, $\boldsymbol{y}_\mathrm{o}$ is the vector of the observations, $\mathbf{B}$, and $\mathbf{R}$ are the background, and observational error covariance matrices, respectively.

The problem can be summarized as the iterative solution of Eq. (1) to find the analysis state $\boldsymbol{x}$ that minimizes $J(\boldsymbol{x})$. This solution represents the a posteriori maximum likelihood (minimum variance) estimate of the true state of the atmosphere given the two sources of a priori data: the background $\boldsymbol{x}_\mathrm{b}$ and observations $\boldsymbol{y}_\mathrm{o}$ (Lorenc, 1986).

For a model state $\boldsymbol{x}$ with $n \sim 10^6$–10^7 degrees of freedom, the direct solution of Eq. (1) is practically unfeasible, because it requires $\sim O(n^2)$ calculations. One practical implementation is to perform a preconditioning via a control variable $\boldsymbol{\chi}$ defined by $\boldsymbol{x}' = \mathbf{U}\boldsymbol{\chi}$, where $\boldsymbol{x}' = \boldsymbol{x} - \boldsymbol{x}_\mathrm{b}$ is the model variable increment. The transform $\mathbf{U}$ is chosen to satisfy the relationship $\mathbf{B} = \mathbf{U}\mathbf{U}^\mathrm{T}$. Using the incremental formulation (Courtier et al., 1994) and the control variable transform, Eq. (1) may be rewritten:

$$J = \frac{1}{2}\boldsymbol{\chi}^\mathrm{T}\boldsymbol{\chi} + \frac{1}{2}\left(\boldsymbol{y}'_\mathrm{o} - \mathrm{H}\mathbf{U}\boldsymbol{\chi}\right)^\mathrm{T}\mathbf{R}^{-1}\left(\boldsymbol{y}'_\mathrm{o} - \mathrm{H}\mathbf{U}\boldsymbol{\chi}\right) \quad (2)$$

where $\boldsymbol{y}'_\mathrm{o} = \boldsymbol{y}_\mathrm{o} - H(\boldsymbol{x}_\mathrm{b})$ is the innovation vector and H is the linearization of the potentially nonlinear observation operator H used in the calculation of $\boldsymbol{y}'_\mathrm{o}$. In this form, the background term is diagonalized, reducing the number of calculations required from $O(n^2)$ to $O(n)$.

The control variable $\boldsymbol{\chi}$ is a vector $\boldsymbol{\chi} = (\boldsymbol{u}', \boldsymbol{v}', \mathrm{RH}', T')$, where $\boldsymbol{u}'$ and $\boldsymbol{v}'$ are the zonal and meridional wind component increments, RH' is the relative humidity increment, and

AMTD
6, 3581–3610, 2013

T' is the temperature increment. The model variable increment $\boldsymbol{x}'$ is a vector $\boldsymbol{x}' = (Z', \boldsymbol{u}', \boldsymbol{v}', \mathrm{RH}', T')$ where Z' is a balanced geopotential height increment, and the other symbols are as in $\boldsymbol{\chi}$.

The transform $\boldsymbol{x}' = \mathbf{U}\boldsymbol{\chi}$ from the control variable $\boldsymbol{\chi}$ to the model variable increment $\boldsymbol{x}'$ is implemented through three operators, namely U_p, U_v, and U_h. The transform U_p is applied after the minimization of the cost function and will be discussed later on in this section; the implementation of U_v and U_h follows that of Barker et al. (2003a, b).

The transform U_h is implemented by recursive filters (Purser et al., 2003). The recursive filter performs the task of convolving a spatial distribution of the innovations with a smoothing kernel, which is the covariance function of the background error. A single pass of a recursive filter consists of an initial advancing smoothing:

$$F_i = (1 - \alpha)D_i + \alpha F_{i-1}$$

for increasing index i, where D is the input forcing and F is the result of the sweep, followed by a backing sweep:

$$R_i = (1 - \alpha)F_i + \alpha R_{i+1}$$

For decreasing i, where F is now the input and R is the response of the filter. The smoothing parameter α is between 0 and 1 and determines the correlation length of the smoothing response function.

The single-pass recursive filter of the operator U_h, involves one smoothing in the WE direction followed by one smoothing in the NS direction.

The recursive filter has two parameters: the number of passes and the length-scale d. The number of passes determines the response of the filter. In particular for $N = 2$ the response approximates a second-order auto-regressive function (SOAR), while for $N = \infty$ the response is Gaussian. In this paper twelve passes are used. This value ensures a well-shaped filter response, without the formation of unphysical lozenge-shaped model variable increment $\boldsymbol{x}'$.

AMTD
6, 3581–3610, 2013

The length-scale of the recursive filters, which determines the smoothing parameter α (see Barker et al., 2003b for the details of the calculation), is computed by the NMC method (Parrish and Derber, 1992). This method gives a climatological estimate of the background error matrix by the averaged difference, computed over a sample, between two short-forecasts verifying at the same time. In this paper a one-month (July 2012) series of 24 h minus 12 h forecasts verifying at 00:00 UTC of each day is used.

The length-scale in the model space is shown in Fig. 1. It depends on the height and on the variable, and it is larger for temperature and smaller for relative humidity. There is an evident increase of the length-scale above the Planetary Boundary Layer (PBL) for all variables. This is expected because the interaction between the orography and the atmospheric flow in the PBL generates features smaller than those of the free atmosphere.

The vertical transform U_v is given by an empirical orthogonal function (EOF) decomposition of the vertical background error matrix ($\mathbf{B}_v$). To determine $\mathbf{B}_v$, the NMC method is applied, by averaging both is space (in longitude and latitude) and time the difference series of 24 h minus 12 h forecasts valid at the same time (see Barker et al., 2003b for a detailed discussion). A one-month time series (July 2012) is used verifying at 00:00 UTC of each day. The $\mathbf{B}_v$ matrix is symmetric and positive-defined and can be decomposed in the eigenvalues and eigenvector matrices, i.e. $\mathbf{B}_v = \mathbf{ELE}^T$, where $\mathbf{E}$ is the eigenvectors and $\mathbf{L}$ the eigenvalues matrix. Using this decomposition, the vertical transform U_v is written as $U_v = \mathbf{EL}^{1/2}$.

To simplify the interpretation of the results, the error correlation between different variables is neglected in this paper and the U_v matrix is a block diagonal matrix, whose blocks are obtained by applying the above decomposition to each variable.

The leading eigenvector of the meridional wind component (Fig. 2), which describes 80 % of the total variance, shows an increasing signal with height and peaks at the jet levels. This result is consistent with the larger wind errors expected at the jet levels. The leading eigenvector of relative humidity, which describes 40 % of the total variance, shows a broad peak in the lower-central troposphere, consistently with the

AMTD
6, 3581–3610, 2013

main portion of the troposphere involved in wet processes in storms development. The temperature leading eigenvector, describing 48 % of the total variance, shows a rather constant profile in the troposphere, which is negatively correlated with errors in the upper troposphere. It should also be mentioned that the second leading eigenvector of temperature, which describe 26 % of the total variance, peaks at 900 hPa showing a strong signal from errors in the planetary boundary layer.

After the minimization of the cost function, the physical transform U_p is applied to transform the control variable $\boldsymbol{\chi} = (\boldsymbol{u}', \boldsymbol{v}', \mathrm{RH}', T')$ to the model variable increments $\boldsymbol{x}' = (Z', \boldsymbol{u}', \boldsymbol{v}', \mathrm{RH}', T')$, which differ only for the balanced geopotential increment.

The balanced geopotential increment is determined by the geostrophic equilibrium in pressure coordinates (the analysis system uses pressure as vertical coordinate, see next section):

$$\nabla_p^2 Z' = \frac{f\xi'}{g} \tag{3}$$

where ξ' is the vertical component of the relative potential vorticity computed from the increments of the zonal (u') and meridional (v') wind components, g is the gravity ($\mathrm{m\,s^{-2}}$) and f is the Coriolis parameter ($\mathrm{s^{-1}}$).

The transform U_p, ensures the balance between the mass and wind increments. A future development of the analysis scheme will involve the implementation of a more sophisticated balance equation improving the mass-wind balance in regions where the geostrophic balance is a coarse approximation of the real flow, as the tropics or the PBL.

Figure 3 shows the combined effect of the transforms U_p, U_v and U_h. In particular it is shown the longitude-height cross section at 57° N latitude for the meridional velocity increment and for the geopotential height increment determined by a single meridional wind component observation introduced over the Gotland Island ~ (57.5° N, 18° E) at 500 hPa. The final increment is spread vertically by the U_v transform and horizontally by U_h. The U_p transform determines the increment of the geopotential height.

AMTD
6, 3581–3610, 2013

Before concluding this section it is important to consider the observation and background errors (σ_b^2, σ_o^2), which determine the relative weight given to the background and observations in the analysis scheme. It is assumed that the observational errors are uncorrelated with each other, so the matrix **R** in Eq. (2) is a diagonal matrix whose elements are all equal to σ_o^2. The dimensions of the matrix **R** equals the number of measurements available at the analysis time. The value of σ_o^2 is taken from the bibliography (Lazarus et al., 2002; Sashegyi et al., 1993) and it is shown in Federico (2013). More in detail, the observational error is equal for the zonal and meridional wind components. It increases from 2.5 m s^{-1} at 1000 hPa to 4 m s^{-1} at 300 hPa. Then it decreases to 3.5 m s^{-1} at 200 hPa. Above 200 hPa the observational error for the velocity components is held constant. For the relative humidity, the observational error is held constant (10 %) from 1000 hPa to 500 hPa, then it increases to 20 % at 200 hPa. Above 200 hPa the relative humidity is not assimilated. For the temperature, the observational error decreases from 1.8 K at 1000 hPa to 1.0 K at 800 hPa. Then it is held constant up to 500 hPa. The error increases from 1.0 K to 2.0 K between 500 and 300 hPa, and is held constant above this level.

The background error is twice the observational error, i.e. $\sigma_b^2 = 2\sigma_o^2$ for all variables and for all levels. So, it is assumed that the background is less reliable than observations.

3 The experiment set-up

The background and the forecast are issued by the RAMS model (non-hydrostatic), version 6.0. Its physical settings are summarized in Table 1.

The strategy to show the impact of the data assimilation on the analysis and short-term forecast is similar to Federico (2013). However, for the paper readability, most of the discussion is repeated in this section.

An important functionality added to the analysis system, compared to Federico (2013), is the possibility to use the same horizontal coordinate system as RAMS, which

AMTD
6, 3581–3610, 2013

uses a rotated polar stereographic projection, whose pole is near the centre of the domain to minimize the projection distortion (Pielke, 2002). In the vertical direction, RAMS uses the sigma-*z* terrain following coordinate (Pielke, 2002), while the analysis uses pressure.

The possibility to run the analysis on the same horizontal coordinate system of RAMS, eventually with coarsened horizontal resolution to speed-up the analysis, is an important feature. Indeed, in the former set-up, the analysis was performed on a regularly-spaced latitude-longitude grid, whose domain was contained in the domain of the RAMS forecast, which was referred as background run. The analysis was used to initialize a RAMS simulation, referred as forecast-run, whose domain was contained in the analysis domain. This process required two different RAMS set-up for the background and forecast run. The new added feature requires one RAMS configuration only and simplifies the interpolation between the RAMS and analysis grids[1].

Figure 4 shows an analysis example for the zonal wind component. The background has 10 km horizontal resolution and covers the central Europe. Its grid setting is shown in Table 2. The analysis increments are given on the same grid as the background but with halved horizontal resolution (20 km) to speed-up the analysis computation.

RAMS uses thirty-three levels in the vertical. The analysis grid uses twenty-nine pressure levels from 1000 hPa to 50 hPa, spaced every 50 hPa between 800 and 300 hPa, and every 25 hPa below 800 hPa. Above 300 hPa the vertical levels are unevenly spaced with a maximum distance of 25 hPa.

Observations used in this paper are upper-air soundings (both land and ship) inside the analysis domain, and the European wind profiler network. Upper-air soundings reports contain vertical profiles of temperature, relative humidity, wind speed and direction, and pressure and are available at synoptic hours (00:00, 06:00, 12:00, 18:00 UTC)

[1]The option to run the analysis on a regularly spaced longitude-latitude grid is still available to use the ISAN (ISentropic Analysis) package, which is the standard method to initialize RAMS (see the RAMS technical manual available at http://www.atmet.com/html/docs/rams/rams_techman.pdf).

AMTD
6, 3581–3610, 2013

with few exceptions. The European wind profilers network measures the wind speed and direction in the vertical above the instrument and observations are available every one-hour.

Observations were downloaded from the MARS (Meteorological Archive and Retrieval System, see also http://www.ecmwf.int/publications/manuals/mars/) archive of ECMWF (European Centre for Medium Weather range Forecast) and the numerical experiment is performed for the month of July 2012. A quality check of the measurements is performed to discard observations affected by gross errors. In particular, only observations whose difference with the background is under a fixed threshold are used in the analyses. The thresholds considered in this paper are equal for all levels and are the following: 8 m s^{-1} for zonal and meridional wind components, 4 K for temperature and 20 % for relative humidity. The application of this quality check discarded less than 5 % of the observations for all variables.

To quantify the impact of the analysis both on the improvement of the initial state and on the short-term forecast, the following strategy is adopted (Fig. 5). For each day of July 2012 one background run lasting 24 h is made starting at 00:00 UTC. Its initial and boundary conditions are taken, every 6 h, from the 00:00 UTC operational analysis/forecast cycle of ECMWF. These fields are available at 0.25° horizontal resolution.

After 12 h of each run, an analysis is made. The 12:00 UTC was chosen because there are several upper-air soundings and wind profiler reports. Figure 6a shows the number of data available for the analyses for the whole period, while Fig. 4b gives an idea of the distribution of the data inside the domain at an analysis time. It is noticeable that there are more data for the wind components because of the data from the European wind profiler network.

Starting from the analysis time (12:00 UTC), a short-term RAMS forecast, lasting 3 h, is made. For this run; (a) the initial conditions are given by the analyses produced at 12:00 UTC; (b) the boundary conditions after 6 h are the same as the background run.

The root mean square error (RMSE) is computed between the background fields and observations, and between the forecast fields and observations for the whole period.

AMTD
6, 3581–3610, 2013

The comparison of these statistics at the analysis time shows the performance of the data assimilation system; the same comparison for times following the analysis time quantifies the impact of the analyses on the short-term forecast.

Statistics are presented for the zonal and meridional wind components only, because few data are available for other variables after the analysis time. Indeed, temperature and relative humidity, which are measured by upper-air soundings, are available at synoptic times (00:00, 06:00, 12:00, 18:00 UTC) with few exceptions, while wind observations are available every one-hour by wind profiler measurements. For example, Fig. 6b shows the number of data at 13:00 UTC for the whole period. Less than 5 observations are available for temperature and relative humidity at all levels, while the number of data for the wind components varies from 309 (875 hPa) to 25 (130 hPa). From Fig. 6 it is apparent that statistics for temperature and relative humidity are reliable only at the analysis time and they will be shortly discussed in the next section.

4 Results

Hereafter the RMSE computed between the background run and the observations at a fixed time and for the whole period is referred as the background error (RMSE_b). Similarly, the RMSE computed between the forecast run and the observations at a fixed time and for the whole period is referred as the forecast error (RMSE_f). For the computation of both RMSEs, the grid point nearest to the observation is considered and the statistics are computed for the whole domain (Fig. 4).

It should also be emphasized that RMSE_f at the analysis time is computed after the analyses have been used to initialize the RAMS model. So, the difference between the RMSE_b and RMSE_f accounts for the errors introduced by the vertical interpolation between the RAMS and analysis grids.

Figure 7a shows the RMSE for the zonal wind component. The RMSE_b is about 2.0 $m\,s^{-1}$ up to 500 hPa, while it increases above this level reaching a maximum of

AMTD
6, 3581–3610, 2013

$3.4\,m\,s^{-1}$ at 250 hPa. The forecast error at the analysis time (RMSE_f) decreases by more than $1.0\,m\,s^{-1}$ for most levels and RMSE_f is more than halved below 900 hPa.

Similar considerations apply for the meridional wind component (Fig. 7b), whose RMSE_f is $\sim 1.0\,m\,s^{-1}$ lower than RMSE_b for most levels; moreover below 850 hPa the error is more than halved.

For the other parameters (not shown, see Federico, 2013) similar results are obtained, with a significant reduction of the error at the analysis time (30–60 % of the background error). The improvement is comparatively larger at the lower levels.

Even if it is not simple to quantify the performance of the data assimilation scheme because the performance varies with the parameter and with the height, a discussion is provided to clarify the results of Fig. 7.

First it should be noticed that the analyses effectively reduce the error. The analysis RMSE is lowered by 30–50 % of the background value for most levels and for all parameters; for few levels, the RMSE reduction is larger than 50 % of the background value.

The error reduction of 30–50 % of the background value is in reasonable agreement with the setting of the data assimilation system. In particular, considering that the model error σ_b^2 is twice the observational error σ_o^2 at all levels, and for the ideal case of one measurement available at a grid point of the analysis grid, the analysis at this point is closer to the observation than to the background, and the error is more than halved. In particular, for this simple ideal case it can be shown that the analysis error (RMSE_f) is $\sigma_o^2/(\sigma_o^2+\sigma_b^2)$ of the background error (RMSE_b; Kalnay, 2003), with an error reduction of 67 %.

The limit of this simple ideal case is not attained in the application of the analysis system for two main reasons: (a) the difference between RMSE_f and RMSE_b of Fig. 7 accounts for the errors introduced by the vertical interpolation between the analysis and forecast grids. This error increases with height as the distance between vertical levels becomes larger; (b) the observations for each level are usually more than one and the innovations of these measurements, i.e. the differences between the background and

AMTD
6, 3581–3610, 2013

observations, interact with each other, as shown by the analysis increments in Northern Italy and Swiss of Fig. 4b.

It is interesting to consider the impact of the analysis on the short-term forecast.

Figure 8 shows the difference between RMSE_b and RMSE_f for the wind components. A positive difference means that the short-term forecast has a lower error than the background and the wind forecast is effectively improved by using the analyses as initial conditions.

After one hour forecast, the improvement of the performance for the zonal velocity is apparent. In particular, the difference of the RMSE_b and RMSE_f is positive for all levels but 150 and 110 hPa and it is larger than 0.4 $m\,s^{-1}$ for several levels. A useful statistic to represent the impact of the analysis on the short-term forecast is the vertically averaged value of the difference between RMSE_b and RMSE_f. This value is 1.00 $m\,s^{-1}$ for the analysis time and 0.35 $m\,s^{-1}$ for the one-hour forecast. From these values it follows that the use of the analyses effectively reduces the error (35 % of the value at the analysis time) after one-hour forecast.

After two-hours forecast the improvement reduces. The vertical average of the difference between RMSE_b and RMSE_f is 0.15 $m\,s^{-1}$, showing that the improvement after two-hours forecast is a sizeable fraction, i.e. larger than 10 %, of the initial value, and that the analysis is still effective at improving the short-term forecast.

For the three-hours forecast the impact of the analysis on the short-term forecast is negligible in practice. There are several levels for which the difference between RMSE_b and RMSE_f is negative, and its vertical average is 0.04 $m\,s^{-1}$.

Figure 8b shows the same statistics of Fig. 8a for the meridional wind component. The impact of the analysis on the one-hour forecast reduces the error of 0.1–0.6 $m\,s^{-1}$, depending on the level. The improvement after one-hour forecast is slightly better for the meridional wind component compared to the zonal wind component. This is confirmed by the vertical average of the difference between RMSE_b and RMSE_f, which is 0.45 $m\,s^{-1}$. This value must be compared with 1.03 $m\,s^{-1}$ at the analysis time, and shows a positive impact of the analysis on the one-hour forecast.

AMTD
6, 3581–3610, 2013

After two-hours, the improvement is reduced, nevertheless its value is larger than $0.2\,m\,s^{-1}$ for several levels. The vertical average of the difference between RMSE_b and RMSE_f is $0.16\,m\,s^{-1}$, which is still a sizeable fraction (16 %) of its initial value.

After three-hours forecast, the improvement is negligible (2 % of the initial value considering the vertical average of the difference between RMSE_b and RMSE_f), and several levels shows a negative impact of the analysis on the short-term forecast.

From the above results, it can be concluded that, for the setting of this paper, the use of the analysis has a positive impact on the one-hour and two-hours forecast for both wind components.

This result is encouraging because the number of data used in the analysis is small. Moreover, it is in agreement with the numerical experiment settings. Indeed, considering the wind components, which have the largest number of measurements, the number of data used by the analysis is, on average, less than 10 for most levels (Fig. 6a). The corrections introduced by these measurements through the analyses, i.e. the analysis increments, are centred at the observational point and have a radius of influence that depends on height, but which is of the order of 100 km (Fig. 1). The analysis increments are advected downwind of the measurement point in few hours, in agreement with the results of this section. It is expected that, using a larger number of data, the positive impact of the analysis on the short-term forecast would last longer.

5 Conclusions

This paper presents the current state of development of a 3-D-Var analysis system, tailored for the RAMS model, which is computationally fast and can be used in small meteorological centres.

The cost-function is written in the incremental form, which ensures that unbalances introduced by the analysis increments are kept at minimum. For the practical minimization of the cost-function a variable transformation is used, which is composed by two

AMTD
6, 3581–3610, 2013

transforms applied in sequence: the horizontal transform U_h, and the vertical transform U_v.

The horizontal transform U_h is applied through recursive filters, which are computationally fast, while the vertical transform U_v is obtained through the eigenvalues-eigenvectors decomposition of the vertical component of the background error matrix.

The length-scale of the recursive filters and the vertical component of the background error matrix are estimated by the NMC method.

The increment of the geopotential height is computed after the minimization of the cost-function, by applying the geostrophic balance to the wind increments (U_p transform). This ensures the balance between the increments of the mass and wind fields.

A practical example is shown for the analysis/short-term wind forecast (0–3 h). Analyses are produced once a day at 12:00 UTC for July 2012 with a horizontal resolution of 20 km and twenty-nine vertical levels. Observations are tropospheric profiles of wind, temperature and relative humidity from upper-air soundings, and tropospheric wind profiles from the European wind profiler network.

Analyses are effective at reducing the initial model error. The improvement is between 30 % and 60 % of the background error for all parameters for most levels. It was shown that this improvement is in agreement with the data assimilation setting, nevertheless there is a decrease of the performance with increasing height caused by the errors introduced by the vertical interpolation between the RAMS and analysis grids.

The impact of the analyses on the short-term forecast is evaluated for the wind components only, because there are few measurements for other variables.

The results show that the improvement for the one-hour forecast is larger than 30 % of the error reduction at the analysis time for both wind components. The same improvement is larger than 15 % of the error reduction at the analysis time for the two-hours forecast and for both wind components. The (positive) impact of the analysis after three-hours forecast is negligible in practice.

AMTD
6, 3581–3610, 2013

It is concluded that, considering the amount of data used in the data assimilation, the results are encouraging and are in agreement with the set-up of the numerical experiment.

Work is in progress on several aspects of the data assimilation system. In particular, future development will consider the inclusion of measurements coming from different sources and a more sophisticated balance for the U_p transform. Nevertheless, the analysis system and the numerical experiment presented in this work should be of interest for the atmospheric profiling community because it can be applied to OSE and OSSE experiments.

Acknowledgements. Most of the elaborations of this work were performed on the ECMWF supercomputing environment, in the framework of the special project SPITFEDE. I am grateful to the "Aereonautica Militare Italiana" and to the ECMWF for the data and for their support in using the MARS archive.

References

Anderson, J.: An ensemble adjustment Kalman filter for data assimilation, Mon. Weather Rev., 129, 2884–2903, 2001.

Barker, D. M., Huang, W., Guo, Y.-R., and Xiao, Q. N.: A three-dimensional variational data assimilation system for MM5: implementation and initial results, Mon. Weather Rev., 132, 897–914, 2003a.

Barker, D. M., Huang, W., Guo, Y.-R., and Bourgeois, A.: A three-dimensional variational (3-DVAR) data assimilation system for use with MM5, NCAR Tech. Note. NCAR/TN-453 1 STR, 68 pp., available from UCAR Communications, P.O. Box 3000, Boulder, CO 80307, 2003b.

Chen, C. and Cotton, W. R.: A one-dimensional simulation of the stratocumulus-capped mixed layer, Bound.-Lay. Meteorol., 25, 289–321, 1983.

Cotton, W. R., Pielke, Sr., R. A., Walko, R. L., Liston, G. E., Tremback, C. J., Jiang, H., McAnelly, R. L., Harrington, J. Y., Nicholls, M. E., Carrio, G. G., and McFadden, J. P.: RAMS 2001: current satus and future directions, Meteorol. Atmos. Phys., 82, 5–29, 2003.

AMTD
6, 3581–3610, 2013

Courtier, P., Thépaut, J. N., and Hollingsworth, A.: A strategy for operational implementation of 4-D-Var, using an incremental approach, Q. J. Roy. Meteor. Soc., 120, 1367–1387, 1994.
Federico, S.: Preliminary results of a data assimilation system, Atmos. Climate Sci., 3, 61–72, 2013.
Kalnay, E.: Atmospheric Modeling, Data Assimilation and Predictability, Cambridge University Press, Cambridge, UK, 2003.
Ide, K., Courtier, P., Ghil, M., and Lorenc, A. C.: Unified notation for data assimilation: operational, sequential and variational, J. Meteorol. Soc. Jpn., 75, 181–189, 1997.
Lazarus, S. M, Ciliberti, C. M., Horel, J. D., and Brewster, K. A.: Near-real-time applications of a mesoscale analysis system to complex terrain, Weather Forecast., 17, 149–160, 2002.
Lorenc, A. C.: Analysis methods for numerical weather prediction, Q. J. Roy. Meteor. Soc., 112, 1177–1194, 1986.
Mellor, G. and Yamada, T.: Development of a turbulence closure model for geophysical fluid problems, Rev. Geophys. Space Ge., 20, 851–875, 1982.
Molinari, J. and Corsetti, T.: Incorporation of cloud-scale and mesoscale down-drafts into a cumulus parametrization: results of one and three-dimensional integrations, Mon. Weather Rev., 113, 485–501, 1985.
Moninger, W. R., Benjamin, S. G., Jamison, B. D., Schlatter, T. W., Smith, T. L., and Szoke, E. D.: Evaluation of regional aircraft observations using TAMDAR, Weather Forecast., 25, 627–645, 2010.
Otkin, J. A., Hartung, D. C., Turner, D. D., Petersen, R. A., Feltz, W. F., and Janzon, E., Assimilation of surface-based boundary layer profiler observations during a cool-season weather event using an observing system simulation experiment. Part I: analysis impact, Mon. Weather Rev., 139, 2327–2346, 2011.
Parrish, D. F. and Derber, J. C.: The National Meteorological Center's spectral statistical interpolation analysis system, Mon. Weather Rev., 120, 1747–1763, 1992.
Pielke, R. A: Mesoscale Meteorological Modeling, Academic Press, San Diego, 2002.
Polkinghorne, R., Vukicevic, T., and Evans, K. F.: Validation of cloud-resolving model background data for cloud data assimilation, Mon. Weather Rev., 138, 781–795, 2009.
Press, W. H., Teukolsky, S. A., Vetterling, W. T., and Flannery, B. P.: Numerical Recipes in Fortran 77, second edn., Cambridge University Press, Cambridge, 1446 pp., 1992.

AMTD
6, 3581–3610, 2013

Purser, R. J., Wu, W.-S., Parrish, D. F., and Roberts, N. M.: Numerical aspects of the application of recursive filters to variational statistical analysis. Part I: spatially homogeneous and isotropic Gaussian covariances, Mon. Weather Rev., 131, 1524–1535, 2003.

Rabier, F., Järvinnen, H., Klinker, E., Mahfouf, J.-F., and Simmons, A.: The ECMWF operational implementation of four-dimensional variational assimilation. I: experimental results with simplified physics, Q. J. Roy. Meteor. Soc., 126, 1143–1170, 2000.

Sashegyi, D. K., Harms, D. E., Madala, R. V., and Raman, S.: Application of the Bratseth scheme for the analysis of GALE, data using a mesoscale model, Mon. Weather Rev., 121, 207–220, 1993.

Schenkman, A. D., Xue, M., Shapiro, A., Brewster, K., and Gao, J.: The analysis and prediction of the 8–9 May 2007 oklahoma tornadic mesoscale convective system by assimilating WSR-88D and CASA radar data using 3-DVAR, Mon. Weather Rev., 139, 224–246, 2011.

Smagorinsky, J.: General circulation experiments with the primitive equations. Part I, the basic experiment, Mon. Weather Rev., 91, 99–164, 1963.

Walko, R. L., Cotton, W. R., Meyers, M. P., and Harrington, J. Y.: New RAMS cloud microphysics parameterization part I: the single-moment scheme, Atmos. Res., 38, 29–62, 1995.

Walko, R. L., Band, L. E., Baron, J., Kittel, T. G., Lammers, R., Lee, T. J., Ojima, D., Pielke, R. A. Sr., Taylor, C., Tague, C., Tremback, C. J., and Vidale, P. L.: Coupled atmosphere-biosphere-hydrology models for environmental prediction, J. Appl. Met., 39, 931–944, 2000.

Xiang-Yu, H., Qingnong, X., Barker, D. M., Zhang, X., Michalakes, J., Huang, W., Henderson, T., Bray, J., Chen, Y., Ma, Z., Dudhia, J., Guo, Y., Zhang, X., Won, D. J., Lin, H. C., and Kuo, Y. H.: Four-dimensional variational data assimilation for WRF: formulation and preliminary results, Mon. Weather Rev., 137, 299–314, doi:10.1175/2008MWR2577.1, 2009.

Zhang, F., Meng., Z., and Askoy, A.: Tests of an ensemble Kalman filter for mesoscale and regional-scale data assimilation. Part I: perfect model experiments, Mon. Weather Rev., 134, 722–736, 2005.

Zupanski, M., Zupanski, D., Vukicevic, T., Eis, K., and Vonder Haar, T.: CIRA/CSU four-dimensional variational data assimilation system, Mon. Weather Rev., 133, 829–843, 2005.

AMTD
6, 3581–3610, 2013

Table 1. RAMS model physical settings.

Physical option	Description
Parametrized cumulus convection	Modified Kuo scheme to account for updraft and downdraft (Molinari and Corsetti, 1985).
Explicit precipitation parametrization	Bulk microphysical model which prognoses cloud water, rain, snow, pristine ice, graupel and hail (Walko et al., 1995).
Subgrid mixing	The turbulent mixing in the horizontal directions is parameterized following Smagorinsky (1963), which relates the mixing coefficients to the fluid strain rate and includes corrections for the influence of the Brunt-Vaisala frequency and the Richardson number (Pielke, 2002). Vertical diffusion is parameterized according to the Mellor and Yamada (1982) scheme, which employs a prognostic turbulent kinetic energy.
Exchange between the surface, the biosphere and the atmosphere.	LEAF-3 sub-model (Walko et al., 2000). LEAF includes prognostic equations for soil temperature and moisture for multiple layers, vegetation temperature and surface water including dew and intercepted rainfall, snow cover mass and thermal energy for multiple layers, and temperature and water vapour mixing ratio of canopy air.
Radiation scheme	A full-column, two-stream single-band radiation scheme is used to calculate short-wave and long-wave radiation (Chen and Cotton, 1983). The Chen and Cotton scheme accounts for condensate in the atmosphere, but not for specific optical properties of ice hydrometeors.

AMTD
6, 3581–3610, 2013

Table 2. RAMS and analysis grid-settings. NNXP, NNYP and NNYZ are the number of grid points in the west-east, north-south, and vertical directions. Lx (km), Ly (km), Lz (m) are the domain extension in the west-east, north-south, and vertical directions. DX (km) and DY (km) are the horizontal grid resolutions in the west-east and north-south directions. CENTLON and CENTLAT are the geographical coordinates of the grid centres. The analysis grid uses pressure as vertical coordinate.

	RAMS grid	Analysis grid
NNXP	231	116
NNYP	231	116
NNZP	32	29
Lx	2520 km	2520 km
Ly	2520 km	2520 km
Lz	18 800 m	1000–50 hPa
DX	10 km	20 km
DY	10 km	20 km
CENTLAT (°)	50.0	50.0
CENTLON (°)	8.0	8.0

AMTD
6, 3581–3610, 2013

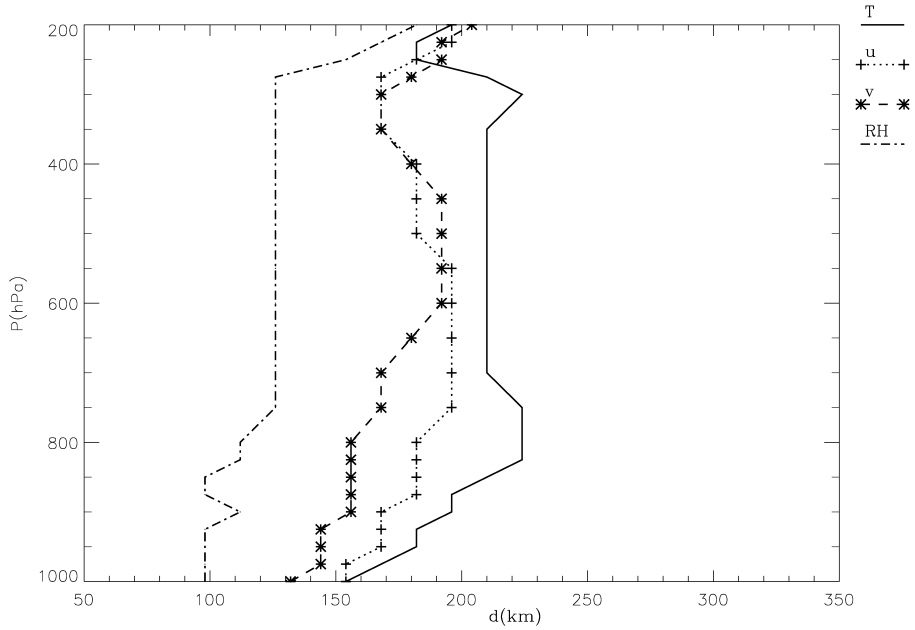

Fig. 1. Length-scale of the different parameters of the control variable as a function of the pressure. *u* is for zonal velocity, *v* is for meridional velocity, *T* is for temperature, and RH is for relative humidity.

AMTD
6, 3581–3610, 2013

Implementation of a 3-D-Var system for atmospheric profiling data assimilation

S. Federico

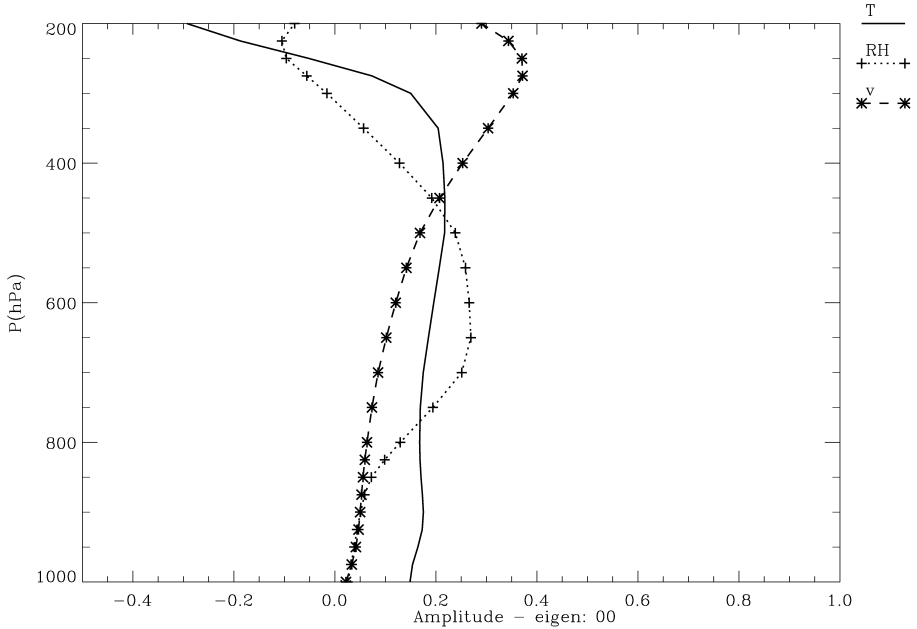

Fig. 2. Leading eigenvector of the meridional wind component (v), temperature (T), and relative humidity (RH). The leading eigenvector for the zonal wind component is similar to that for the meridional wind component and it is not shown for clarity.

AMTD
6, 3581–3610, 2013

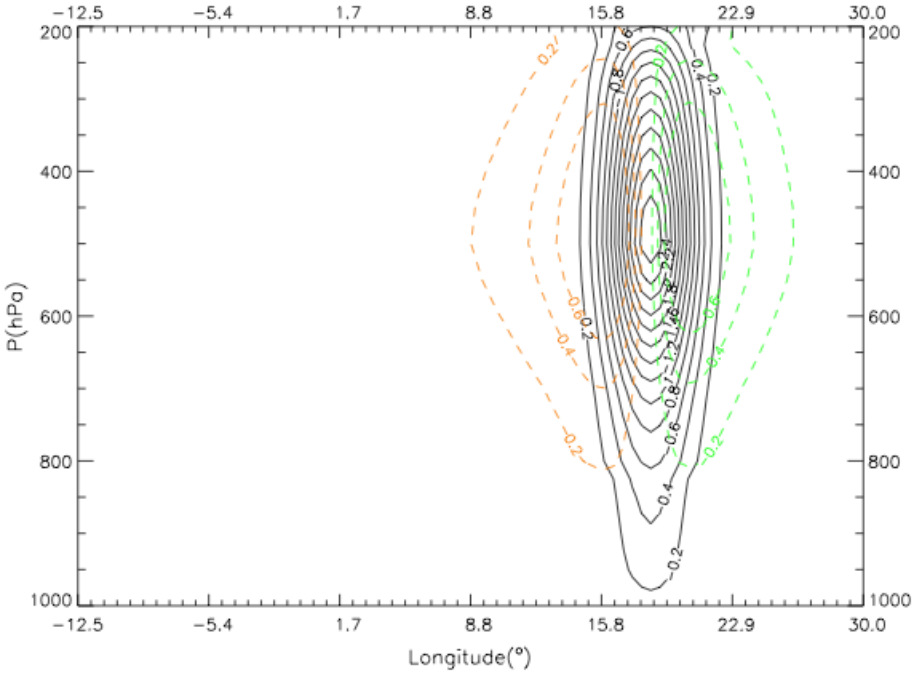

Fig. 3. The effect of the U_h, U_v and U_p transforms (see text for details). Solid lines are contours of meridional wind increments (v', contours from −2.4 to −0.2 m s^{-1} with 0.2 interval); dashed lines are the geopotential height increments Z' (negative to the East and positive to the West of the observation position, contours from −1.0 to 1.0 m with 0.2 m interval).

AMTD
6, 3581–3610, 2013

Implementation of a 3-D-Var system for atmospheric profiling data assimilation

S. Federico

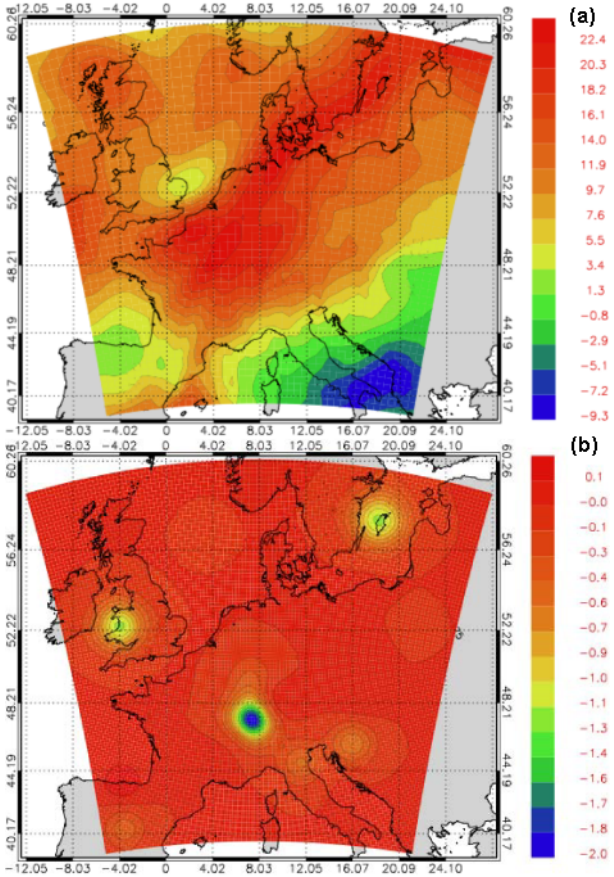

Fig. 4. (a) Background of the zonal wind component ($m s^{-1}$) at 500 hPa at 12:00 UTC on 1 July 2012; **(b)** analysis increments ($m s^{-1}$) at the same time of **(a)**. The figure shows the horizontal domain used in this paper.

AMTD
6, 3581–3610, 2013

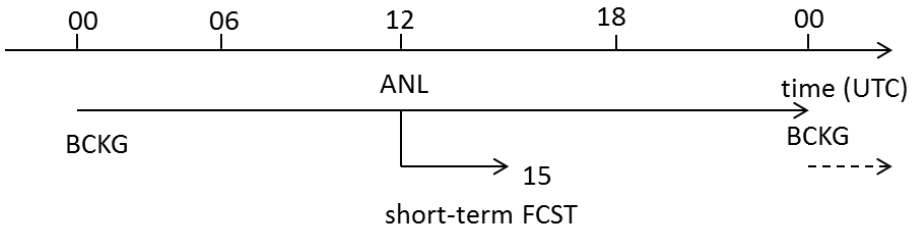

Fig. 5. Synopsis of the simulations. BCKG is the background run, which lasts 24 h. ANL is the analysis time: an analysis is performed at 12:00 UTC. FCST is the short-term forecast, which lasts 3 h.

AMTD
6, 3581–3610, 2013

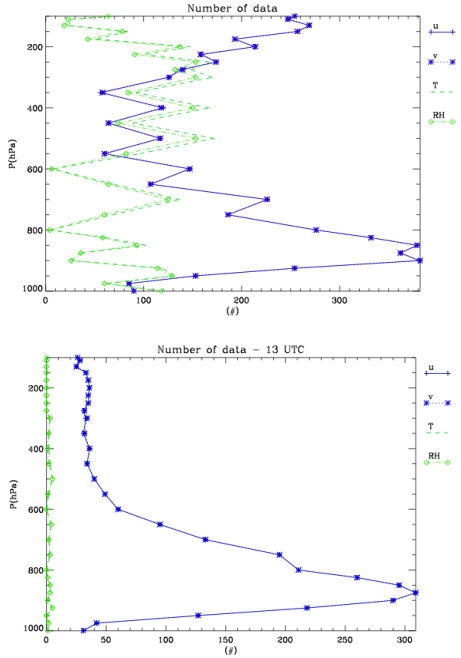

Fig. 6. (a) The number of data available at the analysis time accumulated for the whole period and over the whole domain. T is for temperature, RH is for relative humidity, u and v are for the zonal and meridional wind components, respectively. The number of data for the wind components (u, v) is the same for all levels; **(b)** as in **(a)** for 13:00 UTC.

AMTD
6, 3581–3610, 2013

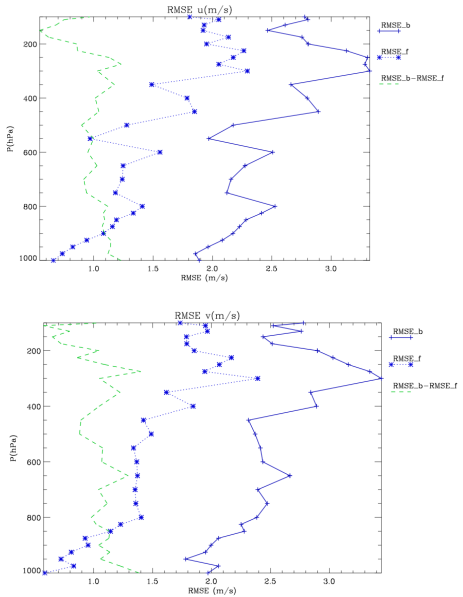

Fig. 7. RMSE of the background field (RMSE_b), of the analyses (RMSE_f), and their difference (RMSE_b-RMSE_f) for: **(a)** zonal wind component; **(b)** meridional wind component. The RMSEs are computed for the whole period considering the grid-points nearest to the observations. The RMSE_f statistics are computed after the RAMS model has been initialized by the analyses.

AMTD
6, 3581–3610, 2013

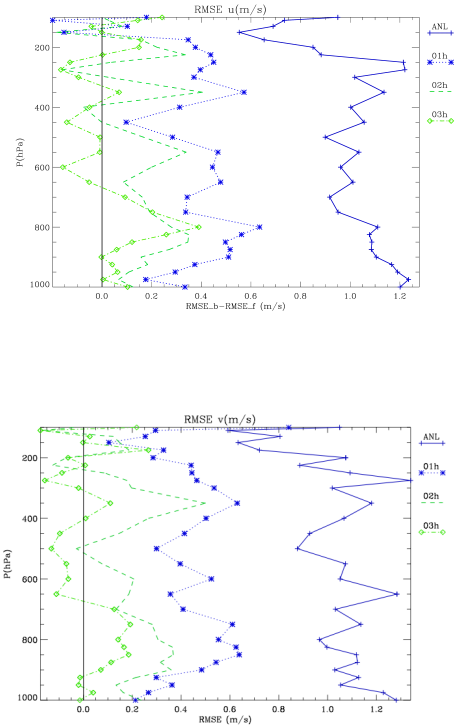

Fig. 8. Differences between RMSE_b and RMSE_f for the analysis time (ANL), one- (1 h), two- (2 h), and three-hours (3 h) forecast for the: **(a)** zonal wind component; **(b)** meridional wind component. The RMSEs are computed for the whole period considering the grid-points nearest to the observations. The analysis time is shown to better understand the behaviour of the performance with time.

AMTD
6, 3581–3610, 2013